iScience

CellPress
OPEN ACCESS

Article

Independent prognostic value of CLDN6 in bladder cancer based on M2 macrophages related signature

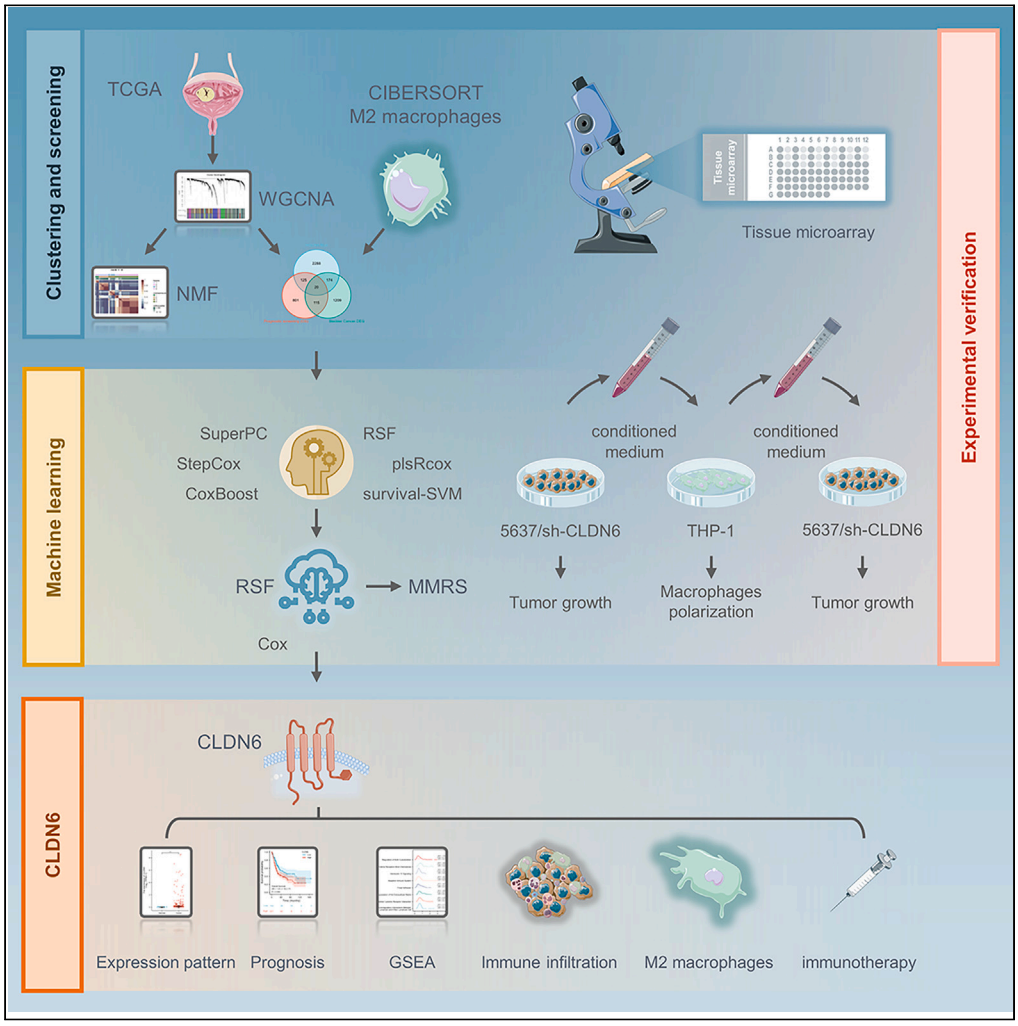

Da Qi, Yan Lu, Huinan Qu, ..., Minghao Sun, Yanru Li, Chengshi Quan

quancs@jlu.edu.cn

Highlights

M2 macrophages related module was identified by WGCNA in bladder cancer

Machine learning was used to construct an M2 macrophages-related signature model

CLDN6 was an independent prognostic risk factor

CLDN6 promoted the polarization of M2 macrophages

Qi et al., iScience 27, 109138
March 15, 2024
https://doi.org/10.1016/j.isci.2024.109138

iScience

CellPress
OPEN ACCESS

Article

Independent prognostic value of CLDN6 in bladder cancer based on M2 macrophages related signature

Da Qi,[1] Yan Lu,[2] Huinan Qu,[3] Yuan Dong,[1] Qiu Jin,[1] Minghao Sun,[1] Yanru Li,[1] and Chengshi Quan[1,4,*]

SUMMARY

M2 macrophages are associated with the prognosis of bladder cancer. CLDN6 has been linked to immune infiltration and is crucial for predicting the prognosis in multi-tumor. The effect of CLDN6 on M2 macrophages in bladder cancer remains elusive. Here, we compared a total of 40 machine learning algorithms, then selected optimal algorithm to develop M2 macrophages-related signature (MMRS) based on the identified M2 macrophages related module. MMRS predicted the prognosis better than other models and associated to immunotherapy response. CLDN6, as an important variable in MMRS, was an independent factor for poor prognosis. We found that CLDN6 was highly expressed and affected immune infiltration, immunotherapy response, and M2 macrophages polarization. Meanwhile, CLDN6 promoted the growth of bladder cancer and enhanced the carcinogenic effect by inducing polarization of M2 macrophages. In total, CLDN6 is an independent risk factor in MMRS to predict the prognosis of bladder cancer.

INTRODUCTION

As the second most common malignant tumor of the urinary system, bladder cancer has a poor prognosis.[1,2] With the increasing understanding of cytological aspects of bladder cancer, the identification of cell signatures and different types of cell populations can help better predict patient outcomes. In particular, the prognostic value of immune cell infiltration in bladder cancer has attracted more and more attention.[3] In recent years, several immunotherapy regimens for bladder cancer have been explored, such as immune checkpoint inhibitors.[4–6] However, there are still some difficult problems in clinical practice, such as how to select the right patients for personalized treatment, and how to predict prognosis and evaluate the therapeutic effect in advance. To address these challenges, there is an urgent need for large-scale, high-precision algorithms, such as machine learning, that can accurately predict prognosis and immunotherapy response.[7]

Tumor-associated macrophages (TAMs) are important components of many tumor types in the immune microenvironment and are often associated with the efficacy and prognosis of immunotherapy.[8,9] In particular, M2 macrophages are enriched in bladder cancer with higher histological grade and pathological stage. Furthermore, patients with higher infiltration degree of M2 macrophages have lower survival rate and a worse effect of immunotherapy.[10,11] M2 macrophages polarization is an important event in the establishment of the tumor immune microenvironment.[12] At the same time, the tumor immune microenvironment and tumor cells themselves also regulate the infiltration of M2 macrophages in turn,[9] so it is necessary to determine the specific factors affecting M2 macrophages and further explore the prognostic value of M2 macrophages.

CLDN6, one of the 27 members of the Claudin (CLDN) family, not only plays the role of classical barriers and fences, but also participates in communication and signaling in a variety of tumor cells.[13] CLDN6 has different expression patterns in different tumors, which leads to its different biological functions. It has been shown that CLDN6 is expressed in bladder cancer but not normal bladder tissue, and patients with high expression of CLDN6 have a poor prognosis.[14,15] In addition, CLDN6 has been found to be associated with immune infiltration in ovarian cancer.[16] However, the evidence linking CLDN6 to M2 macrophages in bladder cancer is still insufficient.

In this study, we compared a total of 40 machine learning algorithms, and then selected optimal algorithm to develop M2 macrophages-related signature (MMRS) based on the identified M2 macrophages related module. MMRS predicted the prognosis better than other models and associated to immunotherapy response. CLDN6 was an important variable in MMRS and screened as an independent poor prognostic factor in bladder cancer. We systematically investigated the expression pattern of CLDN6 in bladder cancer and analyzed the correlation between the expression of CLDN6 and immune infiltration. We also found that CLDN6 promoted the growth of bladder cancer and enhanced the carcinogenic effect by inducing polarization of M2 macrophages. These results extend the application of M2 macrophages in the biology and prognosis prediction of bladder cancer and propose that CLDN6 can be used as a potential predictive biomarker for bladder cancer prognosis and immunotherapy efficacy.

[1]The Key Laboratory of Pathobiology, Ministry of Education, College of Basic Medical Sciences, Jilin University, 126 Xinmin Avenue, Changchun 130021, China
[2]The Department of Anatomy, College of Basic Medical Sciences, Jilin University, 126 Xinmin Avenue, Changchun 130021, China
[3]Department of Histology and Embryology, College of Basic Medical Sciences, Jilin University, 126 Xinmin Avenue, Changchun 130021, China
[4]Lead contact
*Correspondence: quancs@jlu.edu.cn
https://doi.org/10.1016/j.isci.2024.109138

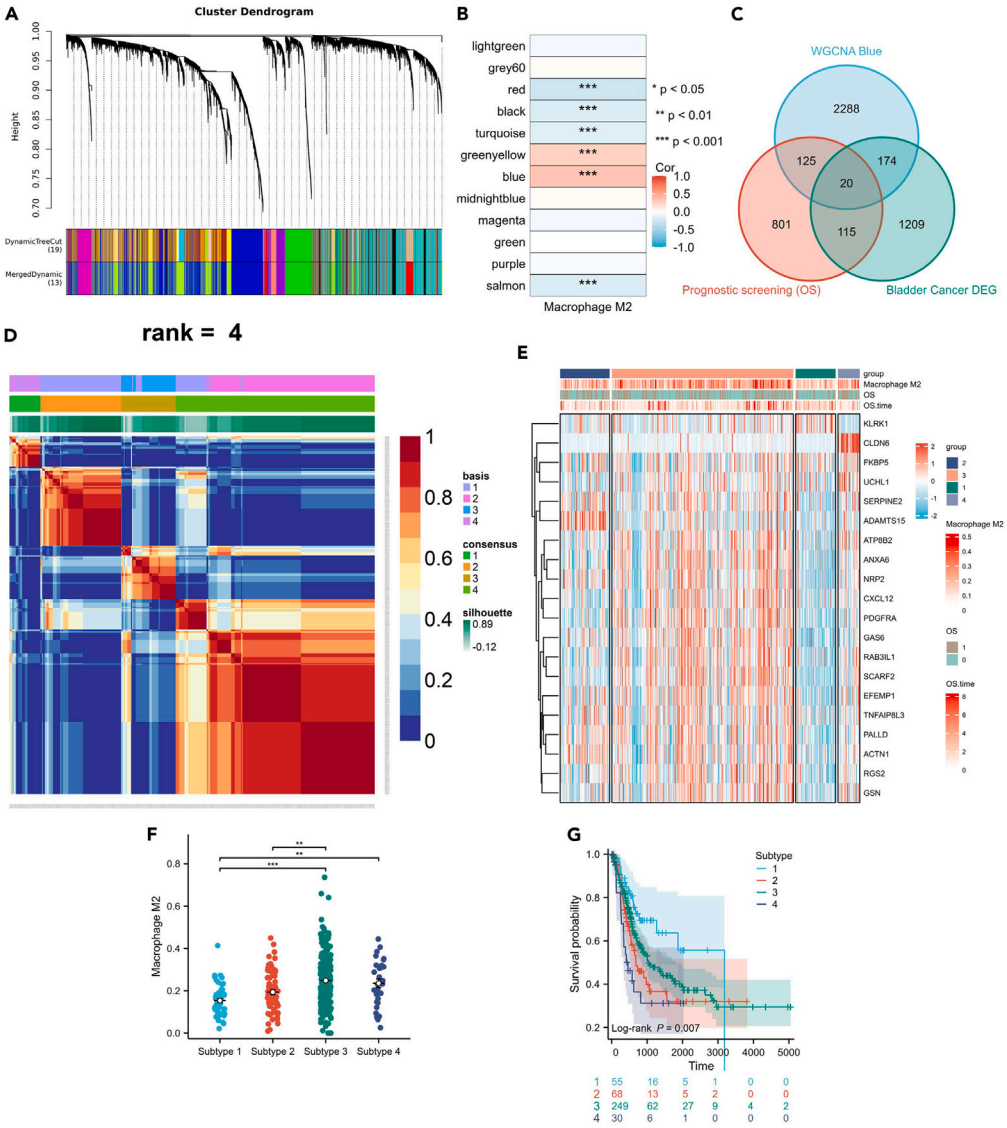

Figure 1. Identification of M2 macrophages related module

(A) The hierarchical gene dendrogram and module color of WGCNA.

(B) Heatmaps showed that WGCNA identified M2 macrophages infiltration related modules.

(C) Venn diagram shows the intersection of genes in the blue module, genes associated with prognosis, and differential genes between bladder cancer and normal bladder tissue.

(D and E) NMF method was used for clustering.

(F) Infiltration of M2 macrophages between different subtypes.

(G) Survival analysis between different subtypes. Data are represented as mean ± SEM.**p < 0.01, ***p < 0.001.

RESULTS

Identification of M2 macrophages related module

First, we used the CIBERSORT algorithm to assess the fraction of M2 macrophages infiltration in the BLCA cohort of TCGA. Kaplan-Meier analysis showed that there was no significant difference between the high and low M1 macrophages infiltration groups in survival (Figure S1A), but patients survived longer in the low M2 macrophages infiltration group (Figure S1B). Considering the significance of M2 macrophages infiltration level on the prognosis of bladder cancer, outliers were eliminated and WGCNA was used to detect the related modules of M2 macrophages infiltration estimated by CIBERSORT. We selected the soft threshold power $\beta = 8$ (scale free $R^2 = 0.85$) to construct a scale-free network (Figure S1C). As the results showed, 12 gene co-expression modules were identified using the dynamic tree cut method (Figure 1A). The heatmap and scatterplots showed that the blue module was positively correlated with the infiltration of M2 macrophages

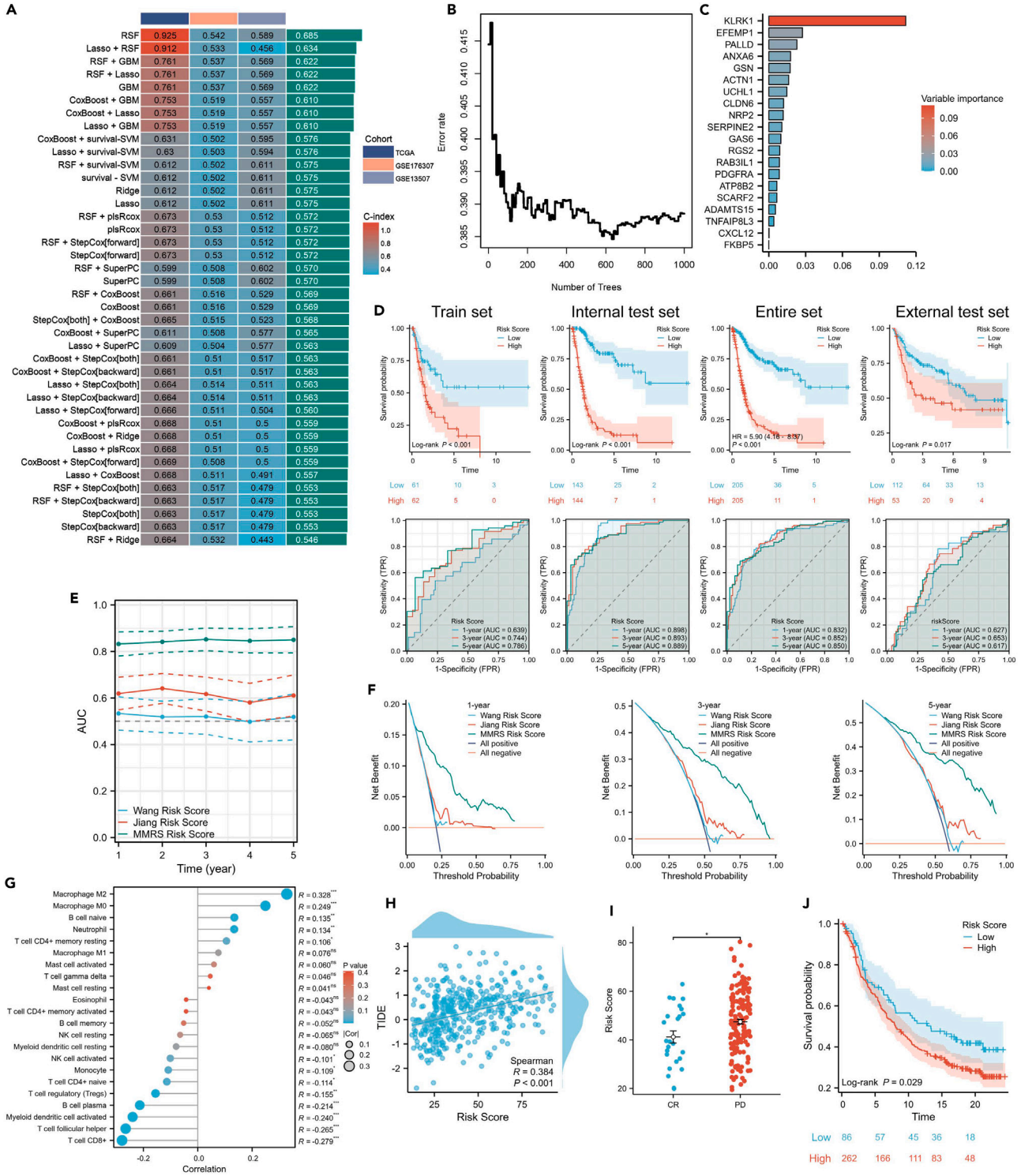

Figure 2. Construct an M2 macrophages-related signature model

(A) A total of 40 kinds of prediction models via LOOCV framework and further calculated the C-index of each model across all validation datasets.

(B) Twenty variables were included in the random forest model, and as the number of trees increased, the error rate gradually stabilized between 0.385 and 0.390.

(C) The importance of 20 variables when predicting OS.

(D) Survival analysis and time-dependent ROC curves for each dataset.

(E) Time-dependent AUC analysis of MMRS versus other models.

Figure 2. *Continued*

(F) DCA graphically illustrated that MMRS brought more net benefit of survival than other models at three different time points.

(G) The relationship between MMRS and immune infiltration was analyzed using CIBERSORT.

(H) Correlation between MMRS and TIDE.

(I) MMRS of CR and PD patients in the IMvigor210 cohort.

(J) Survival analysis of MMRS in IMvigor210 cohort. Data are represented as mean ± SEM. *p < 0.05.

in bladder cancer (Figures 1B and S1D). We performed a univariate Cox regression analysis of survival information in the BLCA cohort of TCGA using genes from the blue module, and intersected with differential genes from bladder cancer and normal bladder tissue. Venn diagram showed that 20 genes were present in the three-way intersection (Figure 1C).

Based on 20 genes, we used the non-negative matrix factorization (NMF) algorithm to classify patients into four subtypes (Figure S1E). The heatmap showed the detailed expression of 20 genes in each subtype (Figures 1D and 1E). We found that the infiltration of M2 macrophages was mainly distributed in subtypes 3 and 4 (Figure 1F). The results of the Kaplan-Meier analysis showed that there were significant differences in the survival of patients with four subtypes, among which the prognosis of patients with subtypes 2, 3, and 4 was worse, and the prognosis of patients with subtype 1 was better (Figure 1G).

Construct an M2 macrophages-related signature model

Next, these 20 genes were subjected to our machine learning-based integrative procedure to develop a consistent MMRS. In the BLCA cohort of The Cancer Genome Atlas (TCGA), we fitted 40 prediction models and further calculated the C-index of each model on all validation datasets. Interestingly, the optimal model was the random survival forest with the highest average c-index, and this model had a leading c-index in all validated datasets (Figure 2A). Subsequently, The BLCA cohort of TCGA was randomly divided into the training set and the internal test set in a ratio of 3–7. MMRS models were constructed for these 20 genes using the random survival forest approach and their relative importance was ranked (Figures 2B and 2C). Using the MMRS model, we calculated a risk score for each patient and found that patients with higher risk scores had worse outcomes in both the training set and the internal test set. Time-dependent survival receiver operating characteristic (ROC) curve of risk score was created to predict 1-, 3-, and 5-year survival rates. It was found that risk score had strong efficiency in predicting patient survival. In addition, using the GSE13507 dataset as an external test set, we found that the risk score calculated by the MMRS model was an adverse prognostic factor for bladder cancer patients (Figure 2D). We also compared two published M2 macrophages-based prognostic models in bladder cancer,[17,18] and time-dependent area under curve (AUC) analysis showed that MMRS had higher predictive power (Figure 2E). Decision curve analysis (DCA) showed that MMRS had the highest net benefit compared with other models when predicting overall survival (OS) at 1, 3, and 5 years (Figure 2F).

Interestingly, the risk score was also associated with the infiltration of multiple immune cells in bladder cancer tissues, among which there was a strong positive correlation with the infiltration of M2 macrophages (Figure 2G). M2 macrophages are strongly associated with immunotherapy effects,[19] so we used the TIDE algorithm to predict potential immunotherapy responses. We found a positive association between risk score and TIDE score, indicating that risk score implied poor immunotherapy effects (Figure 2H). At the same time, in a real immunotherapy IMvigor210 cohort, we analyzed bladder patients with CR (complete response) and PD (progressive disease) after immunotherapy, and found that the risk score was higher in PD patients (Figure 2I). Meanwhile, patients with higher risk scores had shorter overall survival (Figure 2J).

Expression of CLDN6 and relationship with clinicopathological characteristics in bladder cancer

We performed Cox regression analysis on these 20 genes and found that KLRK1 and CLDN6 were independent risk factors affecting the prognosis of patients with bladder cancer (Table S1). KLRK1 is an activated immune receptor expressed by natural killer (NK) and effector T cells. Immunotherapeutic strategies targeting KLRK1 and its ligands can exert antitumor effects through multiple mechanisms such as macrophages polarization.[20] However, the effect of CLDN6 on macrophages polarization and immunotherapy has not been reported. We conducted a systematic study on the role of CLDN6 in bladder cancer.

In order to explore the possible carcinogenic effect of CLDN6 in bladder cancer, we first extracted TCGA data corresponding to bladder urothelial carcinoma and normal tissue data corresponding to GTEx to analyze the expression of CLDN6. Compared with normal samples, CLDN6 was highly expressed in bladder cancer (Figure 3A). We next evaluated the expression of CLDN6 in tumor samples from 15 bladder cancer patients by immunohistochemical staining of the tissue microarray. We found that CLDN6 was highly expressed in bladder cancer compared with its paired paracancerous tissues, and predominantly localized to the membrane of bladder cancer (Figures 3B and 3C). Next, we analyzed the expression pattern of CLDN6 in bladder cancer patients with different clinicopathological characteristics. The results showed that CLDN6 was more highly expressed in non-papillary carcinoma and high-grade patients. Moreover, CLDN6 expression was higher in PD patients compared with CR patients. There was no significant difference in the expression of CLDN6 in patients with different gender, age, TNM stage, pathological stage, and lymphovascular invasion (Figure 3D). In 40 bladder cancer patients with tissue microarray, we found that CLDN6 expression was higher at pathological stage T3 and T4 and clinical stage 3 and 4 (Figures 3E and 3F). These results indicated that CLDN6 was highly expressed in bladder cancer and is associated with various clinicopathological parameters.

CLDN6 is an independent adverse prognostic factor in bladder cancer

Kaplan-Meier (KM) survival analysis was used to evaluate the prognostic value of CLDN6 in bladder cancer. We found that the patients with high expression of CLDN6 showed a lower OS, a poorer disease specific survival (DSS), and progress free interval (PFI), indicating that the

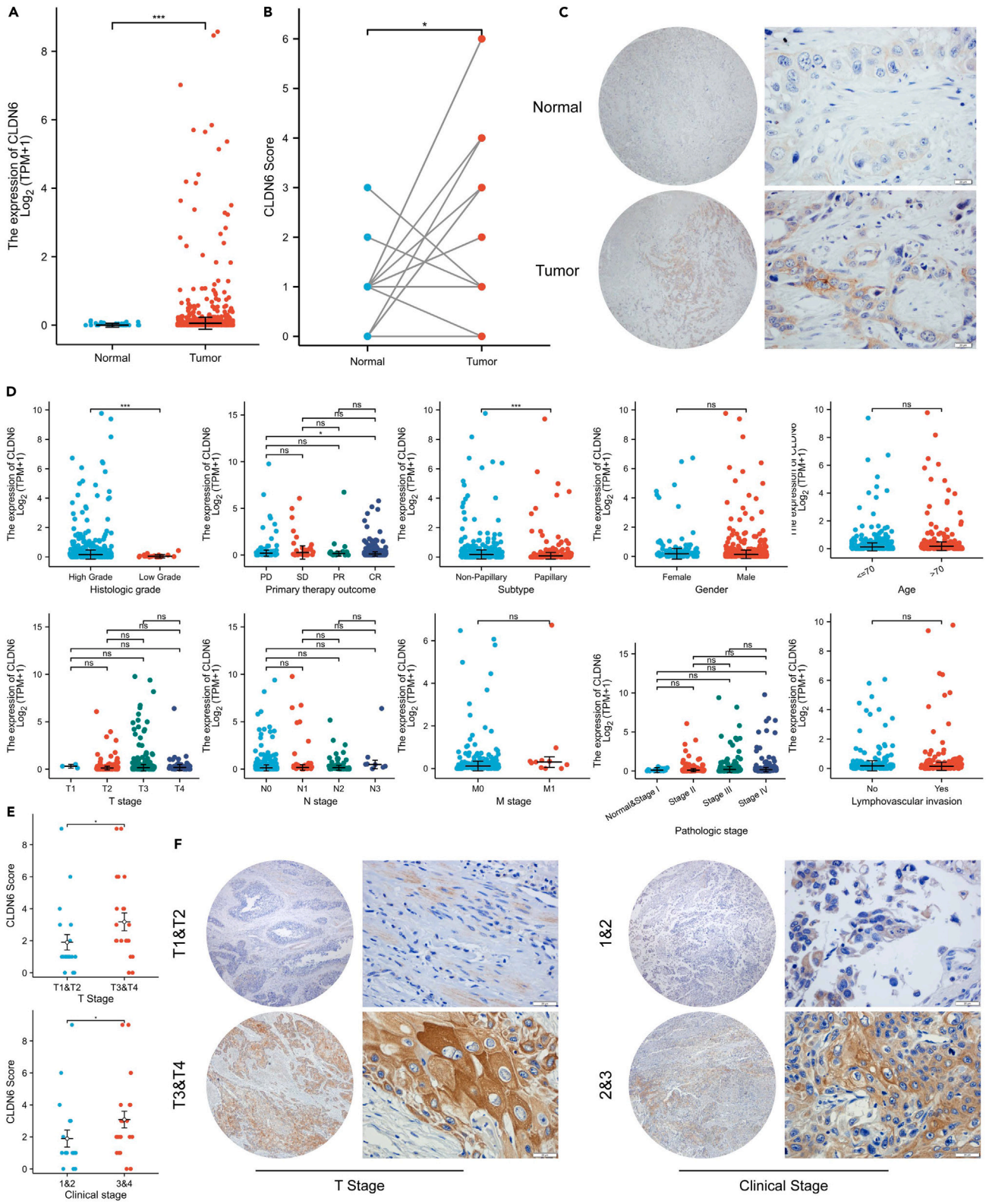

Figure 3. Expression of CLDN6 and relationship with clinicopathological characteristics in bladder cancer

(A) CLDN6 expression in TCGA bladder cancer tissues and normal tissues corresponding to GTEx.

(B) Expression of CLDN6 in adjacent normal tissue and bladder cancer tissue with tissue microarray.

Figure 3. *Continued*

(C) Representative IHC images of CLDN6 in paracancer and bladder cancer. Scale bar, 200 μm (left), 20 μm (right).

(D) Expression of CLDN6 in patients with different clinicopathological parameters.

(E) Expression of CLDN6 in patients with different T stages and clinical stages.

(F) Representative IHC images of CLDN6 in patients with different T stages and clinical stages. Scale bar, 200 μm (left), 20 μm (right). ns, no significance, *$p < 0.05$, ***$p < 0.001$.

prognosis of patients with high expression of CLDN6 was poor (Figure 4A). In addition, patients with high expression of CLDN6 had worse OS and DSS in different subtypes and different pathological grades (except for DSS in patients with papillary bladder cancer) (Figures 4B and S2A). In patients with tissue microarray, we also found the negative effect of CLDN6 on OS (Figure 4C).

The time-dependent survival ROC curve of CLDN6 was created to predict 1-, 3-, and 5-year survival rates. It was found that CLDN6 had low efficacy in predicting patient survival. Surprisingly, CLDN6 could predict the 1-year, 3-year, and 5-year survival rate of patients with tissue microarray (Figure 4D). Additionally, a univariate Cox survival analysis indicated that TNM stage, pathologic stage, subtype, and CLDN6 expression were significant parameters that affect the survival time of bladder cancer patients (Figure 4E). Multivariate Cox survival analysis revealed that N stage and CLDN6 expression were independent predictors of unfavorable prognosis in bladder cancer patients (Figure 4F). Further, calculation of regression coefficient variance inflation factors (VIF) validated that multicollinearity was not an issue (all VIFs <10) (Table S2). All covariates showed no statistical significance, indicating proportional hazard (PH) assumption is true (Table S3). The scaled Schoenfeld residual plot showed that each covariate did not change with time (Figure S2B). To identify the predictive value of the TNM stage, pathologic stage, subtype, and CLDN6 expression, we used nomograms to predict the 1-, 2-, and 3-year OS. As shown, this nomogram was able to assess several variables to predict a patient outcome, which is based on patient characteristics, including TNM stage, pathologic stage, subtype, and CLDN6 expression (Figures 4G and 4H). Additionally, the predictive accuracy for OS was shown by the calibration curves. A calibration curve for the predictive probability showed an accordant agreement for the 1-, 2-, and 3-year OS (Figure 4I). Overall, our results suggested that CLDN6 was an adverse prognostic factor and independent prognostic marker.

GSEA analyzed pathways associated with CLDN6 co-expression genes

To explore the potential molecular function of CLDN6 in bladder cancer, we conducted gene set enrichment analysis (GSEA) analysis between samples with low and high CLDN6 expression to predict CLDN6-related signaling pathways. As shown in the volcano plot, red dots showed significant positive correlations with CLDN6, whereas blue dots showed significant negative correlations (Figure 5A). This result suggested a widespread impact of CLDN6 on the transcriptome. Then we carried out GSEA analysis, and the results showed significant enrichment in the immunoregulatory interactions between a lymphoid and a non-lymphoid cell, cytokine-cytokine receptor interaction, degradation of the extracellular matrix, focal adhesion, adaptive immune system, interleukin 10 signaling, chemokine receptors bind chemokines and regulation of actin cytoskeleton, etc (Figures 5B and 5C). Intriguingly, most of the enrichment pathways were correlated with immune infiltration. Taken together, it was necessary to comprehensively analyze the oncogenic role of CLDN6 in the immune infiltration of bladder cancer patients.

Role of CLDN6 in immune infiltration and immunotherapy response

The single-sample gene set enrichment analysis (ssGSEA) analysis was used to comprehensively assess the correlations between CLDN6 expression and a panel of immune infiltrates in bladder cancer. The results demonstrated that the expression level of CLDN6 positively correlated with infiltrating levels of macrophages, Th2 cells, Th1 cells, Tgd cells, TFH, Tem, NK cells, neutrophils, B cells, and eosinophils in bladder cancer but negatively correlated with Tcm, Th17 cells, and T helper cells (Figure 5D). CIBERSORT analysis showed that CLDN6 expression correlated with immune cells, including M2 macrophages, M0 macrophages, resting mast cells, regulatory T cells, resting mast cells, resting myeloid dendritic cells, monocytes, plasma B cells and naive B cells (Figure 5E). Unfortunately, in bladder cancer patients with tissue microarray, we found no statistically significant correlation between CLDN6 and CD8+%, a marker of killer T cells, probably because of the limitation of patient sample size (Figure 5F). Altogether, the aforementioned results indicated that CLDN6 might be involved in the immune infiltration in bladder cancer.

MSI is an important predictive biomarker for immunotherapy response.[21] Next, we investigated whether there was a correlation between the expression level of CLDN6 and MSI. We found that CLDN6 was significantly negatively correlated with the MSI score in bladder cancer tissue (Figure 5G). In addition, CLDN6 expression was found to be positively correlated with TIDE scores, indicating that CLDN6 might be an adverse factor for the efficacy of immunotherapy (Figure 5H).

CLDN6 promotes the growth of bladder cancer and enhances the carcinogenic effect by inducing polarization of M2 macrophages

In the immune infiltration analysis, we found that M2 macrophages had a high degree of infiltration, rather than M1 macrophages in bladder cancer tissues with high expression of CLDN6 (Figure 6A). This suggests that CLDN6 might affect the polarization of M2 macrophages. To further confirm the association between CLDN6 and different macrophages subtypes, we investigated the correlation of CLDN6 and the markers of M1 and M2 macrophages, as well as TAMs in bladder cancer. The results showed that the correlation between M1 macrophages markers (such as PTGS2 and NOS2) and the expression of CLDN6 was weak, while the gene markers of M2 macrophages (such as CD163, MRC1, and MS4A4A) were significantly positive correlation with CLDN6, and the TAMs markers (such as CD86, CCL2, and IL10) were also correlated with the level of CLDN6 (Figures 6B and S3A).

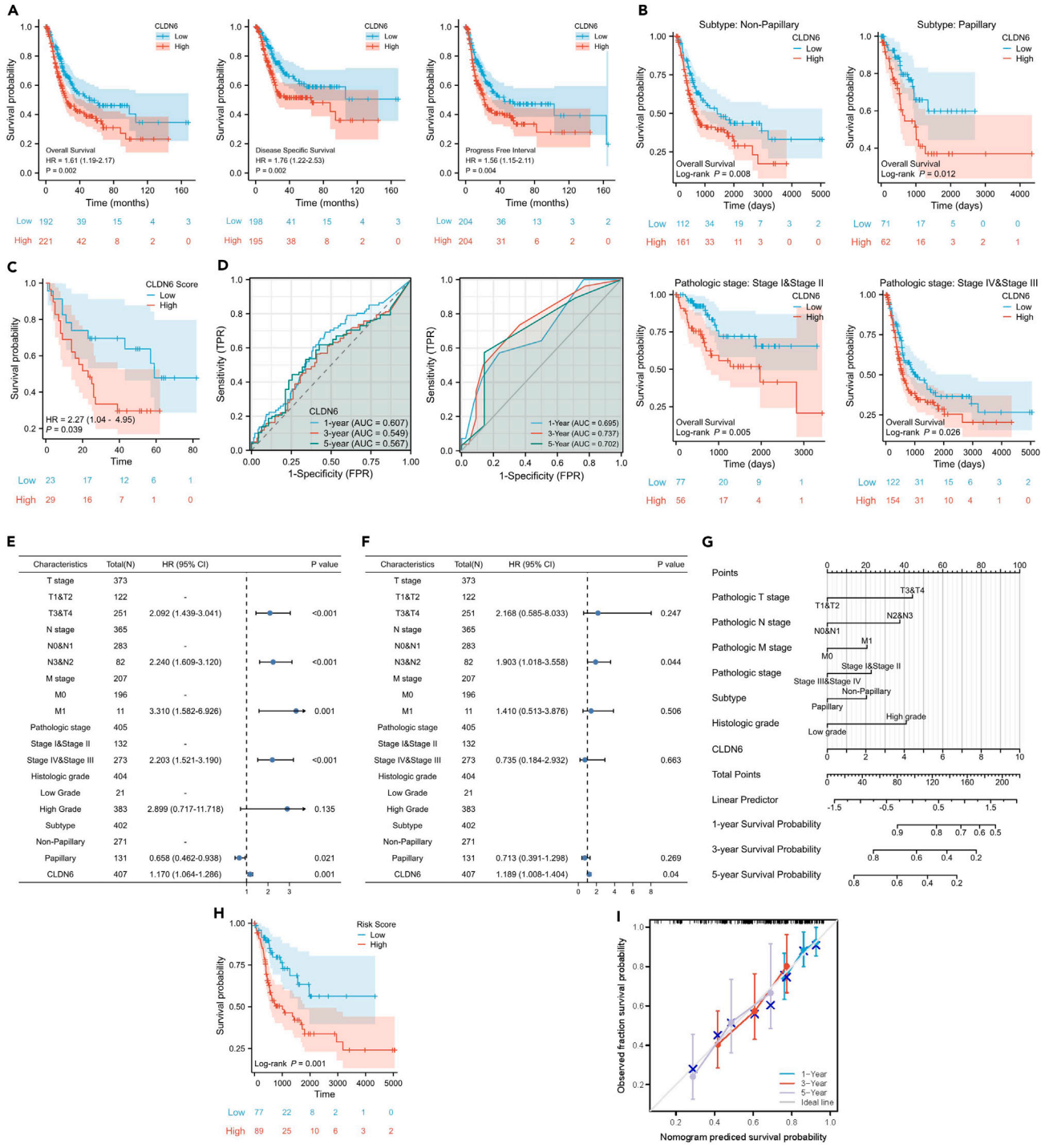

Figure 4. CLDN6 is an independent adverse prognostic factor in bladder cancer

(A) Survival analysis showed the relationship between CLDN6 and OS, DPS, and PFI.

(B) The prognostic value of CLDN6 in different subtypes of bladder cancer.

(C) Tissue microarray was used to analyze the prognostic value of CLDN6 in bladder cancer patients.

(D) Time-dependent ROC curves of CLDN6 in TCGA bladder cancer cohort and tissue microarray.

(E) Forest plots showed Cox univariate regression analysis of CLDN6.

(F) Forest plots showed Cox multivariate regression analysis of CLDN6.

(G) The nomogram was used to estimate the 1-, 3-, and 5-year survival probabilities by integrating independent prognostic measures.

(H and I) the Prognostic value of the nomogram.

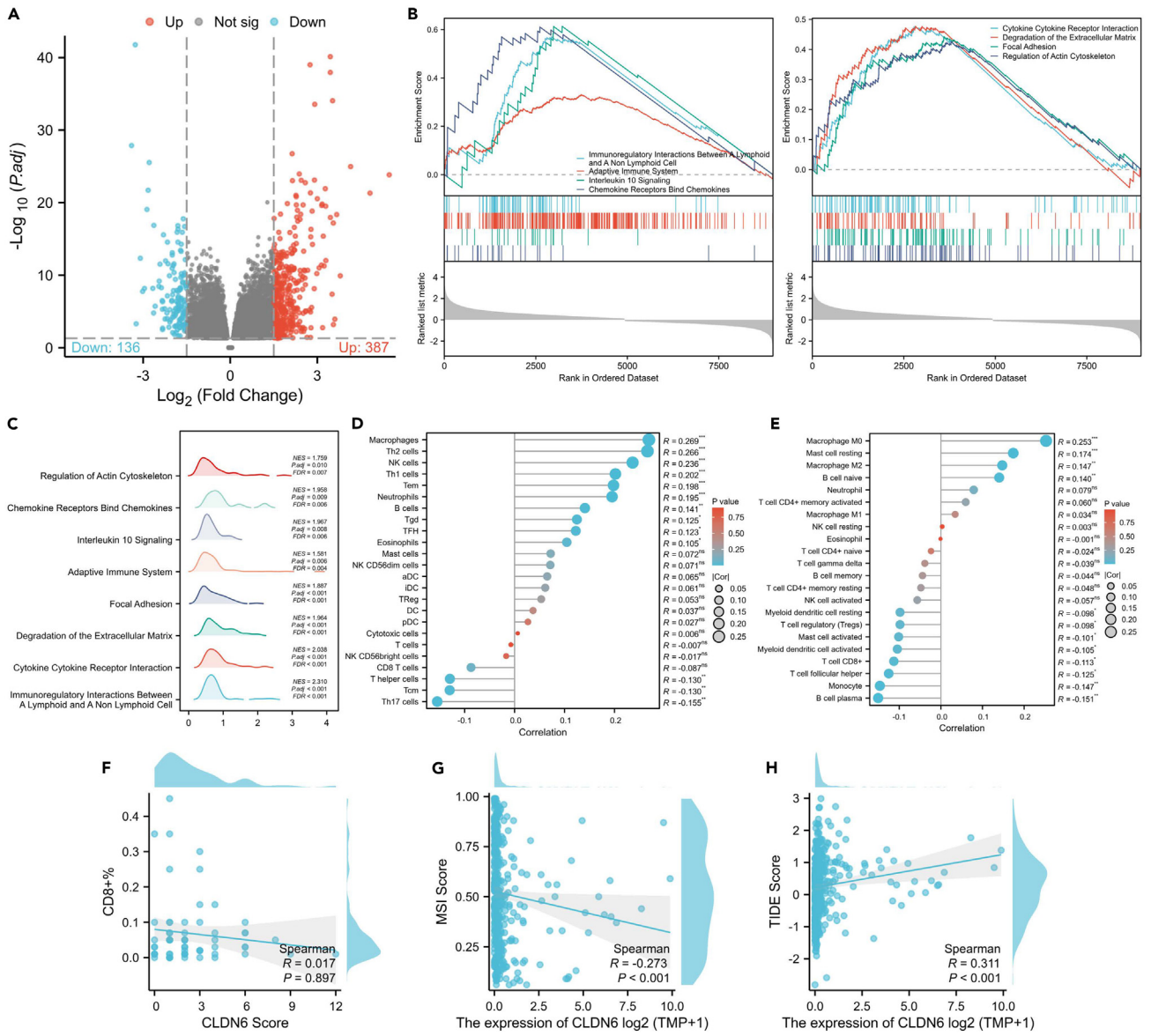

Figure 5. GSEA analyzed pathways associated with CLDN6 co-expression genes, and the role of CLDN6 in immune infiltration and immunotherapy effect

(A) Volcanic maps showed CLDN6 co-expressing genes.

(B and C) GSEA analysis revealed pathways enriched by CLDN6 co-expressed genes.

(D) ssGSEA was used to analyze the relationship between CLDN6 and immune infiltration.

(E) CIBERSORT was used to analyze the relationship between CLDN6 and immune infiltration.

(F) Correlation between CLDN6 and CD8+%.

(G) Correlation between CLDN6 and MSI.

(H) Correlation between CLDN6 and TIDE.

To further verify the effect of CLDN6 on M2 macrophages polarization, we next evaluated the expression of CLDN6, CD163, and NOS2 in tumor samples from 40 bladder cancer tissue microarray by IHC staining (Figure 6C). Spearman correlation analyses indicated that CLDN6 and CD163 were positively correlated. CLDN6 expression was not significantly correlated with NOS2 in bladder cancer tissues (Figure 6D). Altogether, these results indicated that CLDN6 promote M2 macrophages polarization in bladder issues.

To clarify the effect of CLDN6 on macrophage polarization, we first silenced CLDN6 in bladder cancer cells and examined the silencing efficiency (Figures 6E and S3B). Then, western blot (WB) and immunofluorescence (IF) were used to detect the polarization of macrophages. The results showed that conditioned medium (CM) from sh-CLDN6 bladder cancer cells inhibited the expression of CD163 and increased

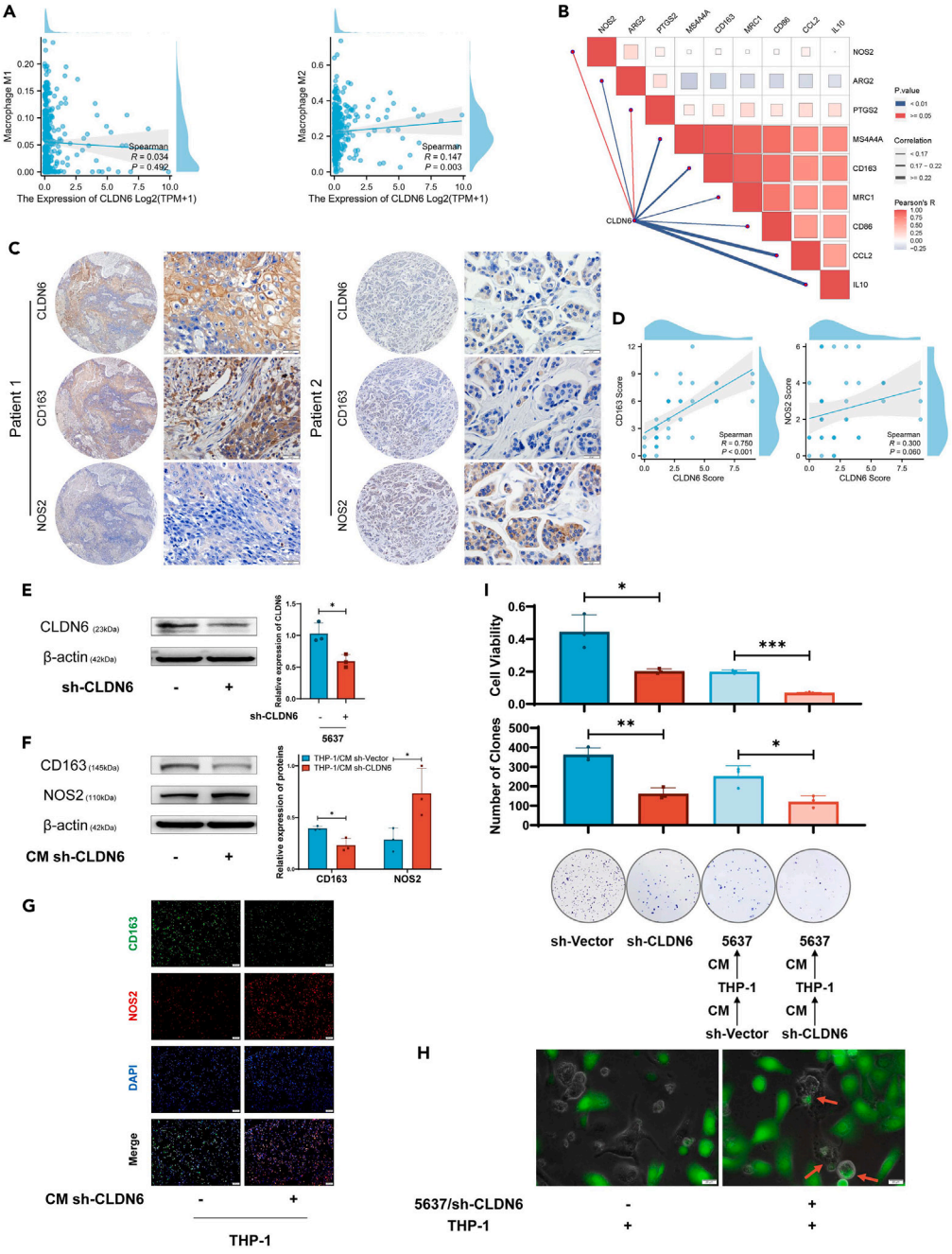

Figure 6. CLDN6 is associated with M2 macrophages polarization

(A) Correlation of CLDN6 with M1 and M2 macrophages.

(B) Correlation between CLDN6 and markers of M1, M2 macrophages and TAMs.

(C) Representative IHC images of CLDN6, CD163, and NOS2 in bladder cancer.

(D) Correlation of CLDN6 with CD163 and NOS2. Scale bar, 200 μm (left), 20 μm (right).

(E and F) CLDN6, CD163, and NOS2 expression levels in the whole cell lysate from the indicated cells were assessed using WB.

(G) CD163 and NOS2 in the indicated cells were observed using fluorescent microscopy. Green: CD163; red: NOS2; blue: DAPI. Scale bar: 200 μm.

(H) Macrophages were co-cultured with bladder cancer cells. Bladder cancer cells engulfed by macrophages are indicated by red arrows, Scale bar: 20 μm.

(I) Cell viability was determined using CCK-8 and plate cloning assay. Data are represented as mean ± SEM. *p < 0.05, **p < 0.01, ***p < 0.001.

the level of NOS2 in macrophages (Figures 6F and 6G). Furthermore, we found that phagocytosis of macrophages was increased when co-cultured with sh-CLDN6 bladder cancer cells (Figure 6H). This suggested that CLDN6 induced polarization of M2 macrophages and inhibited their phagocytosis. We further investigated the effects of CLDN6 and its induced macrophage polarization on growth in bladder cancer. Our results suggested that silencing CLDN6 reduced the viability and number of clones of bladder cancer cells. In addition, the macrophage CM induced by sh-CLDN6 bladder cancer cells inhibited the growth of bladder cancer cells (Figure 6I). The aforementioned results showed that CLDN6 promoted the growth of bladder cancer and enhanced the carcinogenic effect by inducing polarization of M2 macrophages.

DISCUSSION

Due to the rapid progression and high recurrence rate of bladder cancer, the prognosis of patients is still not optimistic.[22] In recent years, a lot of research has been devoted to the prognosis of patients with bladder cancer.[23–26] Studies have shown that abnormal gene expression of bladder cancer cells and immune infiltration in the tumor microenvironment may be involved in the occurrence and prognosis.[27,28] However, there is an urgent need for more advanced algorithms such as machine learning to predict prognosis and immunotherapy response in bladder cancer. In this study, we established an MMRS by machine learning in bladder cancer and screened out an independent prognostic factor, CLDN6. Furthermore, we investigated the role of CLDN6 in the prognosis, immune infiltration, immunotherapy response, and M2 macrophages polarization in bladder cancer.

Recent studies have demonstrated that M2 macrophages are associated with a poorer prognosis in bladder cancer.[17,29] Macrophages in bladder cancer tissues mostly exhibit an M2-like phenotype, and M2 macrophages have been found to promote the growth and development of bladder cancer by inhibiting inflammation.[30] Meanwhile, there is a study using machine learning to construct a model based on M2 macrophage infiltration, which can predict the immunotherapy response in bladder cancer.[19] In addition to the stimulation of a series of factors such as IL-4, the process of macrophages polarization toward M2 is also regulated by a variety of factors produced by tumor cells themselves.[30,31] There is a lack of reliable model to predict prognosis in bladder cancer patients. In this study, we used WGCNA to explore key modules related to M2 macrophages infiltration in bladder cancer, and based on the expression profiles of 20 selected genes, we constructed a consensus MMRS. Among the 40 machine learning models, we selected the optimal random survival forest model and found that MMRS was a detrimental factor for the prognosis of patients with bladder cancer. In addition, we found that MMRS was positively correlated with the infiltration of M2 macrophages in bladder cancer tissues and could predict the response of patients to immunotherapy. At present, several studies have explored prognostic models based on the infiltration of M2 macrophages in bladder cancer. The Cox regression model developed by Wang et al. for four M2 macrophages co-expressed genes can predict the survival of bladder cancer patients.[18] Moreover, Jiang et al. used LASSO-Cox regression to establish a prognosis model related to M2 macrophages and found that this model may be a potential prognostic marker for bladder cancer.[17] We compared the predictive efficacy of the aforementioned two models with the MMRS established in this study and found that the predictive efficacy of MMRS was better than the aforementioned two models.

In this study, we performed Cox regression analysis on genes in MMRS and found that CLDN6 was an independent risk factor. CLDN6 is a member of the tight junction protein family and is expressed abnormally in a variety of tumors.[13] The expression of CLDN6 has been identified as an important prognostic factor in a variety of tumors.[32–35] There is evidence that CLDN6 is highly expressed in bladder cancer and is associated with poor prognosis in patients.[14,15] Here we further analyzed the expression and prognostic value of CLDN6 in patients with different clinical parameters, and found that CLDN6 was highly expressed in bladder cancer and correlated with the histological grade, subtype, and main treatment outcome of patients. We also found that CLDN6 was an independent risk factor for the prognosis of patients with bladder cancer. In addition, we verified the results by immunohistochemistry in bladder cancer tissue microarray. Here, for the first time, we systematically analyzed the effectiveness and independence of CLDN6 in predicting prognosis in patients with bladder cancer.

Numerous studies have shown that immune infiltration is an important factor affecting the prognosis of bladder cancer patients.[36] Our GSEA analysis of CLDN6 co-expressed genes revealed that CLDN6 may be involved in multiple immune-related pathways. Studies have shown that CLDN6 expression correlates with immune cell infiltration in ovarian cancer.[16] The relationship between CLDN6 and immune infiltration in bladder cancer remains unclear. Our study showed that CLDN6 is involved in the immune infiltration in bladder cancer. In bladder cancer patients with tissue microarray, we found no statistically significant correlation between CLDN6 and CD8+%, probably because of the limitation of the patient sample size. In particular, CLDN6 is positively correlated with M2 macrophages polarization, and CLDN6 may be an adverse factor affecting the response to immunotherapy. CLDN5 has been reported to be positively correlated with macrophage infiltration in bladder cancer,[37] but there is still no evidence that CLDN6 affects macrophages. Here we describe for the first time that CLDN6 induces polarization of M2 macrophages and inhibits their phagocytosis in bladder cancer. CLDN6 not only promotes tumor growth, but also enhances carcinogenesis by inducing M2 macrophage polarization.

In conclusion, we established an MMRS by screening 40 machine learning algorithms, in which CLDN6, an independent prognostic risk factor, predicted the prognosis by promoting the polarization of M2 macrophages in bladder cancer. Our study expands the understanding of the role of M2 macrophages in the biology and prognostic prediction of bladder cancer, and provides evidence for CLDN6 as a new predictive biomarker for prognosis and immunotherapeutic efficacy in bladder cancer.

Limitations of the study

The main limitation of our research is the lack of experiments *in vitro* and *in vivo* to explore the regulation of CLDN6 on macrophages polarization and immunotherapy. The clinical utility of the MMRS required independent validation in a larger pool of patients with bladder cancer.

STAR★METHODS

Detailed methods are provided in the online version of this paper and include the following:

- KEY RESOURCES TABLE
- RESOURCE AVAILABILITY
  - Lead contact
  - Materials availability
  - Data and code availability
- EXPERIMENTAL MODEL AND STUDY PARTICIPANT DETAILS
  - Cell lines and cell culture
  - Human samples
  - Study participant details
- METHOD DETAILS
  - Dataset source and preprocessing
  - Functional enrichment analysis and estimation of immune infiltration
  - Weighted gene co-expression network analysis (WGCNA)
  - Non-negative matrix factorization (NMF) clustering
  - Machine learning
  - M2 macrophages-related signature construction and validation
  - Predicting the efficacy of immunotherapy
  - Gene set enrichment analysis
  - Immunohistochemistry (IHC)
  - Western blot (WB)
  - Immunofluorescence (IF)
  - Cell counting kit-8 (CCK-8)
  - Plate clone formation assay
  - Medical illustrations
- QUANTIFICATION AND STATISTICAL ANALYSIS

SUPPLEMENTAL INFORMATION

Supplemental information can be found online at https://doi.org/10.1016/j.isci.2024.109138.

ACKNOWLEDGMENTS

The authors would like to thank the Key Laboratory of Pathology, Jilin University for providing experimental equipment and technical support. This study was funded by the National Natural Science Foundation of China (grant no. 82072935) and the Science and Technology Development Projects of Jilin Province (grant no. 20220402083GH).

AUTHOR CONTRIBUTIONS

C.Q. and D.Q. conceived and designed the study. D.Q. drafted the manuscript. D.Q., Y.Lu., and H.Q. performed most of the experiments. Y.D. and Q.J. collected and analyzed data. M.S. and Y.Li. proofread the manuscript. All authors read and approved the final manuscript.

DECLARATION OF INTERESTS

The authors declare no competing interests.

Received: August 9, 2023
Revised: December 19, 2023
Accepted: February 1, 2024
Published: February 5, 2024

REFERENCES

1. Compérat, E., Amin, M.B., Cathomas, R., Choudhury, A., De Santis, M., Kamat, A., Stenzl, A., Thoeny, H.C., and Witjes, J.A. (2022). Current best practice for bladder cancer: a narrative review of diagnostics and treatments. Lancet *400*, 1712–1721. https://doi.org/10.1016/s0140-6736(22)01188-6.
2. Alifrangis, C., McGovern, U., Freeman, A., Powles, T., and Linch, M. (2019). Molecular and histopathology directed therapy for advanced bladder cancer. Nat. Rev. Urol. *16*, 465–483. https://doi.org/10.1038/s41585-019-0208-0.
3. van Wilpe, S., Gerretsen, E.C.F., van der Heijden, A.G., de Vries, I.J.M., Gerritsen, W.R., and Mehra, N. (2020). Prognostic and Predictive Value of Tumor-Infiltrating Immune Cells in Urothelial Cancer of the Bladder. Cancers (Basel) *12*, 2692. https://doi.org/10.3390/cancers12092692.
4. Song, D., Powles, T., Shi, L., Zhang, L., Ingersoll, M.A., and Lu, Y.J. (2019). Bladder cancer, a unique model to understand cancer immunity and develop immunotherapy approaches. J. Pathol. *249*, 151–165. https://doi.org/10.1002/path.5306.
5. Patel, V.G., Oh, W.K., and Galsky, M.D. (2020). Treatment of muscle-invasive and advanced bladder cancer in 2020. CA. Cancer J. Clin. *70*, 404–423. https://doi.org/10.3322/caac.21631.
6. Lenis, A.T., Lec, P.M., Chamie, K., and Mshs, M.D. (2020). Bladder Cancer: A Review. Jama *324*, 1980–1991. https://doi.org/10.1001/jama.2020.17598.
7. Chu, G., Ji, X., Wang, Y., and Niu, H. (2023). Integrated multiomics analysis and machine learning refine molecular subtypes and prognosis for muscle-invasive urothelial cancer. Mol. Ther. Nucleic Acids *33*, 110–126. https://doi.org/10.1016/j.omtn.2023.06.001.
8. Xiang, X., Wang, J., Lu, D., and Xu, X. (2021). Targeting tumor-associated macrophages to synergize tumor immunotherapy. Signal Transduct. Target. Ther. *6*, 75. https://doi.org/10.1038/s41392-021-00484-9.
9. Leblond, M.M., Zdimerova, H., Desponds, E., and Verdeil, G. (2021). Tumor-Associated Macrophages in Bladder Cancer: Biological Role, Impact on Therapeutic Response and Perspectives for Immunotherapy. Cancers (Basel) *13*, 4712. https://doi.org/10.3390/cancers13184712.
10. Xue, Y., Tong, L., LiuAnwei Liu, F., Liu, A., Zeng, S., Xiong, Q., Yang, Z., He, X., Sun, Y., and Xu, C. (2019). Tumor-infiltrating M2 macrophages driven by specific genomic alterations are associated with prognosis in bladder cancer. Oncol. Rep. *42*, 581–594. https://doi.org/10.3892/or.2019.7196.
11. Li, Z., Wu, T., Zheng, B., and Chen, L. (2019). Individualized precision treatment: Targeting TAM in HCC. Cancer Lett. *458*, 86–91. https://doi.org/10.1016/j.canlet.2019.05.019.
12. Shields, C.W., 4th, Evans, M.A., Wang, L.L.W., Baugh, N., Iyer, S., Wu, D., Zhao, Z., Pusuluri, A., Ukidve, A., Pan, D.C., and Mitragotri, S. (2020). Cellular backpacks for macrophage immunotherapy. Sci. Adv. *6*, eaaz6579. https://doi.org/10.1126/sciadv.aaz6579.
13. Qu, H., Jin, Q., and Quan, C. (2021). CLDN6: From Traditional Barrier Function to Emerging Roles in Cancers. Int. J. Mol. Sci. *22*, 13416. https://doi.org/10.3390/ijms222413416.
14. Ushiku, T., Shinozaki-Ushiku, A., Maeda, D., Morita, S., and Fukayama, M. (2012). Distinct expression pattern of claudin-6, a primitive phenotypic tight junction molecule, in germ cell tumours and visceral carcinomas. Histopathology *61*, 1043–1056. https://doi.org/10.1111/j.1365-2559.2012.04314.x.
15. Zhang, C., Guo, C., Li, Y., Liu, K., Zhao, Q., and Ouyang, L. (2021). Identification of Claudin-6 as a Molecular Biomarker in Pan-Cancer Through Multiple Omics Integrative Analysis. Front. Cell Dev. Biol. *9*, 726656. https://doi.org/10.3389/fcell.2021.726656.
16. Gao, P., Peng, T., Cao, C., Lin, S., Wu, P., Huang, X., Wei, J., Xi, L., Yang, Q., and Wu, P. (2021). Association of CLDN6 and CLDN10 With Immune Microenvironment in Ovarian Cancer: A Study of the Claudin Family. Front. Genet. *12*, 595436. https://doi.org/10.3389/fgene.2021.595436.
17. Jiang, Y., Qu, X., Zhang, M., Zhang, L., Yang, T., Ma, M., Jing, M., Zhang, N., Song, R., Zhang, Y., et al. (2022). Identification of a six-gene prognostic signature for bladder cancer associated macrophage. Front. Immunol. *13*, 930352. https://doi.org/10.3389/fimmu.2022.930352.
18. Wang, Y., Yan, K., Wang, J., Lin, J., and Bi, J. (2021). M2 Macrophage Co-Expression Factors Correlate With Immune Phenotype and Predict Prognosis of Bladder Cancer. Front. Oncol. *11*, 609334. https://doi.org/10.3389/fonc.2021.609334.
19. Wang, J., He, X., Bai, Y., Du, G., and Cai, M. (2022). Identification and validation of novel biomarkers affecting bladder cancer immunotherapy via machine learning and its association with M2 macrophages. Front. Immunol. *13*, 1051063. https://doi.org/10.3389/fimmu.2022.1051063.
20. Fuertes, M.B., Domaica, C.I., and Zwirner, N.W. (2021). Leveraging NKG2D Ligands in Immuno-Oncology. Front. Immunol. *12*, 713158. https://doi.org/10.3389/fimmu.2021.713158.
21. Yang, Y., Jain, R.K., Glenn, S.T., Xu, B., Singh, P.K., Wei, L., Hu, Q., Long, M., Hutson, N., Wang, J., et al. (2020). Complete response to anti-PD-L1 antibody in a metastatic bladder cancer associated with novel MSH4 mutation and microsatellite instability. J. Immunother. Cancer *8*, e000128. https://doi.org/10.1136/jitc-2019-000128.
22. Tran, L., Xiao, J.F., Agarwal, N., Duex, J.E., and Theodorescu, D. (2021). Advances in bladder cancer biology and therapy. Nat. Rev. Cancer *21*, 104–121. https://doi.org/10.1038/s41568-020-00313-1.
23. Feng, Z.H., Liang, Y.P., Cen, J.J., Yao, H.H., Lin, H.S., Li, J.Y., Liang, H., Wang, Z., Deng, Q., Cao, J.Z., et al. (2022). m6A-immune-related lncRNA prognostic signature for predicting immune landscape and prognosis of bladder cancer. J. Transl. Med. *20*, 492. https://doi.org/10.1186/s12967-022-03711-1.
24. Xia, Q.D., Sun, J.X., Xun, Y., Xiao, J., Liu, C.Q., Xu, J.Z., An, Y., Xu, M.Y., Liu, Z., Wang, S.G., and Hu, J. (2022). SUMOylation Pattern Predicts Prognosis and Indicates Tumor Microenvironment Infiltration Characterization in Bladder Cancer. Front. Immunol. *13*, 864156. https://doi.org/10.3389/fimmu.2022.864156.
25. Song, Q., Zhou, R., Shu, F., and Fu, W. (2022). Cuproptosis scoring system to predict the clinical outcome and immune response in bladder cancer. Front. Immunol. *13*, 958368. https://doi.org/10.3389/fimmu.2022.958368.
26. Chen, X., Xu, R., He, D., Zhang, Y., Chen, H., Zhu, Y., Cheng, Y., Liu, R., Zhu, R., Gong, L., et al. (2021). CD8(+) T effector and immune checkpoint signatures predict prognosis and responsiveness to immunotherapy in bladder cancer. Oncogene *40*, 6223–6234. https://doi.org/10.1038/s41388-021-02019-6.
27. Luo, Y., Barrios-Rodiles, M., Gupta, G.D., Zhang, Y.Y., Ogunjimi, A.A., Bashkurov, M., Tkach, J.M., Underhill, A.Q., Zhang, L., Bourmoum, M., et al. (2019). Atypical function of a centrosomal module in WNT signalling drives contextual cancer cell motility. Nat. Commun. *10*, 2356. https://doi.org/10.1038/s41467-019-10241-w.
28. Efstathiou, J.A., Mouw, K.W., Gibb, E.A., Liu, Y., Wu, C.L., Drumm, M.R., da Costa, J.B., du Plessis, M., Wang, N.Q., Davicioni, E., et al. (2019). Impact of Immune and Stromal Infiltration on Outcomes Following Bladder-Sparing Trimodality Therapy for Muscle-Invasive Bladder Cancer. Eur. Urol. *76*, 59–68. https://doi.org/10.1016/j.eururo.2019.01.011.
29. Zhang, P.B., Huang, Z.L., Xu, Y.H., Huang, J., Huang, X.Y., and Huang, X.Y. (2019). Systematic analysis of gene expression profiles reveals prognostic stratification and underlying mechanisms for muscle-invasive bladder cancer. Cancer Cell Int. *19*, 337. https://doi.org/10.1186/s12935-019-1056-y.
30. Sharifi, L., Nowroozi, M.R., Amini, E., Arami, M.K., Ayati, M., and Mohsenzadegan, M. (2019). A review on the role of M2 macrophages in bladder cancer; pathophysiology and targeting. Int. Immunopharmacol. *76*, 105880. https://doi.org/10.1016/j.intimp.2019.105880.
31. Kobatake, K., Ikeda, K.I., Nakata, Y., Yamasaki, N., Ueda, T., Kanai, A., Sentani, K., Sera, Y., Hayashi, T., Koizumi, M., et al. (2020). Kdm6a Deficiency Activates Inflammatory Pathways, Promotes M2 Macrophage Polarization, and Causes Bladder Cancer in Cooperation with p53 Dysfunction. Clin. Cancer Res. *26*, 2065–2079. https://doi.org/10.1158/1078-0432.Ccr-19-2230.
32. Song, P., Li, Y., Dong, Y., Liang, Y., Qu, H., Qi, D., Lu, Y., Jin, X., Guo, Y., Jia, Y., et al. (2019). Estrogen receptor β inhibits breast cancer cells migration and invasion through CLDN6-mediated autophagy. J. Exp. Clin. Cancer Res. *38*, 354. https://doi.org/10.1186/s13046-019-1359-9.
33. Kojima, M., Sugimoto, K., Tanaka, M., Endo, Y., Kato, H., Honda, T., Furukawa, S., Nishiyama, H., Watanabe, T., Soeda, S., et al. (2020). Prognostic Significance of Aberrant Claudin-6 Expression in Endometrial Cancer. Cancers (Basel) *12*, 2748. https://doi.org/10.3390/cancers12102748.
34. Yu, S., Zhang, Y., Li, Q., Zhang, Z., Zhao, G., and Xu, J. (2019). CLDN6 promotes tumor progression through the YAP1-snail1 axis in gastric cancer. Cell Death Dis. *10*, 949. https://doi.org/10.1038/s41419-019-2168-y.
35. Kohmoto, T., Masuda, K., Shoda, K., Takahashi, R., Ujiro, S., Tange, S., Ichikawa, D., Otsuji, E., and Imoto, I. (2020). Claudin-6 is a single prognostic marker and functions as a tumor-promoting gene in a subgroup of intestinal type gastric cancer. Gastric Cancer *23*, 403–417. https://doi.org/10.1007/s10120-019-01014-x.
36. Kamoun, A., de Reyniès, A., Allory, Y., Sjödahl, G., Robertson, A.G., Seiler, R.,

Hoadley, K.A., Groeneveld, C.S., Al-Ahmadie, H., Choi, W., et al. (2020). A Consensus Molecular Classification of Muscle-invasive Bladder Cancer. Eur. Urol. *77*, 420–433. https://doi.org/10.1016/j.eururo.2019.09.006.

37. Han, L., Cui, D.J., Huang, B., Yang, Q., Huang, T., Lin, G.Y., and Chen, S.J. (2023). CLDN5 identified as a biomarker for metastasis and immune infiltration in gastric cancer via pan-cancer analysis. Aging (Albany NY) *15*, 5032–5051. https://doi.org/10.18632/aging.204776.
38. Mariathasan, S., Turley, S.J., Nickles, D., Castiglioni, A., Yuen, K., Wang, Y., Kadel, E.E., III, Koeppen, H., Astarita, J.L., Cubas, R., et al. (2018). TGFβ attenuates tumour response to PD-L1 blockade by contributing to exclusion of T cells. Nature *554*, 544–548. https://doi.org/10.1038/nature25501.
39. Yang, M., Li, Y., Shen, X., Ruan, Y., Lu, Y., Jin, X., Song, P., Guo, Y., Zhang, X., Qu, H., et al. (2017). CLDN6 promotes chemoresistance through GSTP1 in human breast cancer. J. Exp. Clin. Cancer Res. *36*, 157. https://doi.org/10.1186/s13046-017-0627-9.
40. Davis, S., and Meltzer, P.S. (2007). GEOquery: a bridge between the Gene Expression Omnibus (GEO) and BioConductor. Bioinformatics *23*, 1846–1847. https://doi.org/10.1093/bioinformatics/btm254.
41. Leek, J.T., Johnson, W.E., Parker, H.S., Jaffe, A.E., and Storey, J.D. (2012). The sva package for removing batch effects and other unwanted variation in high-throughput experiments. Bioinformatics *28*, 882–883. https://doi.org/10.1093/bioinformatics/bts034.
42. Colaprico, A., Silva, T.C., Olsen, C., Garofano, L., Cava, C., Garolini, D., Sabedot, T.S., Malta, T.M., Pagnotta, S.M., Castiglioni, I., et al. (2016). TCGAbiolinks: an R/Bioconductor package for integrative analysis of TCGA data. Nucleic Acids Res. *44*, e71. https://doi.org/10.1093/nar/gkv1507.
43. Rooney, M.S., Shukla, S.A., Wu, C.J., Getz, G., and Hacohen, N. (2015). Molecular and genetic properties of tumors associated with local immune cytolytic activity. Cell *160*, 48–61. https://doi.org/10.1016/j.cell.2014.12.033.
44. Newman, A.M., Liu, C.L., Green, M.R., Gentles, A.J., Feng, W., Xu, Y., Hoang, C.D., Diehn, M., and Alizadeh, A.A. (2015). Robust enumeration of cell subsets from tissue expression profiles. Nat. Methods *12*, 453–457. https://doi.org/10.1038/nmeth.3337.
45. Langfelder, P., and Horvath, S. (2008). WGCNA: an R package for weighted correlation network analysis. BMC Bioinf. *9*, 559. https://doi.org/10.1186/1471-2105-9-559.
46. Hamamoto, R., Takasawa, K., Machino, H., Kobayashi, K., Takahashi, S., Bolatkan, A., Shinkai, N., Sakai, A., Aoyama, R., Yamada, M., et al. (2022). Application of non-negative matrix factorization in oncology: one approach for establishing precision medicine. Brief. Bioinform. *23*, bbac246. https://doi.org/10.1093/bib/bbac246.
47. Bonneville, R., Krook, M.A., Kautto, E.A., Miya, J., Wing, M.R., Chen, H.Z., Reeser, J.W., Yu, L., and Roychowdhury, S. (2017). Landscape of Microsatellite Instability Across 39 Cancer Types. JCO Precis. Oncol. *2017*, 1–15. https://doi.org/10.1200/po.17.00073.
48. Jiang, P., Gu, S., Pan, D., Fu, J., Sahu, A., Hu, X., Li, Z., Traugh, N., Bu, X., Li, B., et al. (2018). Signatures of T cell dysfunction and exclusion predict cancer immunotherapy response. Nat. Med. *24*, 1550–1558. https://doi.org/10.1038/s41591-018-0136-1.

STAR★METHODS

KEY RESOURCES TABLE

REAGENT or RESOURCE	SOURCE	IDENTIFIER
Antibodies		
Mouse anti-CLDN6 monoclonal antibody	Santa Cruz	sc-393671
Mouse anti-CD163 monoclonal antibody	Proteintech	68218-1-Ig
Rabbit anti-NOS2 polyclonal antibody	Proteintech	22226-1-AP
Rabbit anti-β-actin monoclonal antibody	Proteintech	66009-1-Ig
Deposited data		
TCGA-BLCA RNA-seq data	The Cancer Genome Atlas	N/A
Gene expression microarray data	Gene Expression Omnibus (GEO) database	Accession number: GSE176307 and GSE13507
Bulk RNA-seq data from IMvigor210 clinical trial	Banchereau et al.[38]	EGAS00001004343
Experimental models: Cell lines		
5637	Haixing Biosciences	TCH-C104
THP-1	Yanbian University	N/A

RESOURCE AVAILABILITY

Lead contact

Further information and requests for resources should be directed to and will be fulfilled by the lead contact, Chengshi Quan (quancs@jlu.edu.cn).

Materials availability

This study did not generate new unique reagents.

Data and code availability

- All the data corresponding to the bladder cancer dataset used in this study are available in GEO (https://www.ncbi.nlm.nih.gov/geo) and TCGA (https://portal.gdc.cancer.gov/), which are public functional genomics data repositories.
- This paper does not report original code.
- Any additional information required to reanalyze the data reported in this paper is available from the lead contact Chengshi Quan on request.

EXPERIMENTAL MODEL AND STUDY PARTICIPANT DETAILS

Cell lines and cell culture

The human bladder cancer cell line (5637) was obtained from the Haixing Biosciences and the monocytic leukemia cells line (THP-1) was donated by Yanbian University. 5637 and THP-1 were cultured in RPMI-1640 medium (Meilune, China) containing 10% FBS (Gibco, USA) and 1% P/S (100 U/mL penicillin, 100 mg/mL streptomycin) at 37°C in a humidified incubator containing 5% CO_2. THP-1 cells were differentiated into macrophages treated with 100 nM PMA for 24 h, and then cultured with CM from bladder cancer cells or directly co-cultured with bladder cancer cells. The CLDN6 shRNA es were purchased from Genechem. The transfection process was performed as described by Yang et al.[39]

Human samples

Human bladder cancer tissue microarray (TMA; HBlaU079Su01 and HBlaU050CS01) was purchased from Shanghai Outdo Biotech CO. The study was approved by the Ethics Committee of Shanghai Outdo Biotech CO (protocol code YB M-05-02).

Study participant details

CQ and DQ conceived and designed the study. DQ drafted the manuscript. DQ, YL, and HQ performed most of the experiments. YD and QJ collected and analyzed data. MS and YL proofread the manuscript. All authors read and approved the final manuscript.

METHOD DETAILS

Dataset source and preprocessing

The analyses involved patients from four bladder cancer cohorts (GSE176307, GSE13507, and IMvigor210) and the bladder cancer cohort in TCGA. Patients without survival information and RNA sequencing data were excluded from the analysis. For the GEO dataset, related clinical data and transcriptome expression data were downloaded using the R GEOquery package[40] and the related GEO datasets were merged using the ComBat algorithm.[41] Transcriptome FPKM (fragments per kilobase transcript per million fragments) value and clinical data were downloaded from the Genomic Data Commons (GDC, https://portal.gdc.cancer.gov/) using the R TCGA biolinks package.[42] The FPKM values were transformed to TPM (transcripts per million) values for subsequent analyses.

Functional enrichment analysis and estimation of immune infiltration

The levels of 37 immune and tumor-related signatures in each sample were quantified by single-sample gene set enrichment analysis (ssGSEA) with the R package "GSVA".[43] Immune cell infiltration was quantified using the CIBERSORT algorithm based on the TPM value of the bladder cancer cohort in TCGA.[44]

Weighted gene co-expression network analysis (WGCNA)

We constructed mRNA co-expression networks in the bladder cancer cohort of TCGA using the R WGCNA package.[45] First, the Pearson correlation coefficient between each pair of genes was calculated to obtain a similarity matrix. WGCNA converted the similarity matrix to an adjacency matrix using a power function. Among all soft thresholds (β) with $R^2 > 0.85$, we chose the automatic value β (β = 8) returned by the WGCNA pick Soft Threshold function. As recommended by the WGCNA guidelines, 0.25 was chosen as the network merge height. We used default settings for other WGCNA parameters.

Non-negative matrix factorization (NMF) clustering

Non-negative matrix factorization (NMF) is an effective dimensionality reduction method that is widely used to distinguish molecular patterns in high-dimensional genomic data.[46] Patients with bladder cancer were divided into four subtypes based on the expression of 20 genes using the "NMF" R package.

Machine learning

We integrated a total of 40 combinations based on 10 machine learning algorithms. The integrative algorithms included StepCox, random survival forest (RSF), supervised principal components (SuperPC), partial least squares regression for Cox (plsRcox), CoxBoost, survival support vector machine (survival-SVM), Lasso, Ridge, and generalized boosted regression modeling (GBM). MMRS in the TCGA bladder cancer cohort was fitted based on the leave-one-out cross-validation (LOOCV) framework. Harrell's concordance index (C-index) was subsequently calculated in two independent GEO datasets to select an optimal MMRS with the highest C-index.

M2 macrophages-related signature construction and validation

We created a random survival forest (RSF) for the model by using the rfsrc function of the randomForestSRC R package (v2.9.3). A gene combination with the optimal log-rank P value was identified for the signature construction: Risk Score = Σ (βi * Expi), where βi was the ith gene's Cox coefficient, and Expi was the ith gene's expression value. The prognostic value of the MMRS was then validated in GSE13507 and IMvigor210 cohort patients.

Predicting the efficacy of immunotherapy

Tumor Immune Dysfunction and Exclusion (TIDE, https://tide.dfci.harvard.edu/) is a comprehensive score for tumor immune dysfunction and immune escape, including tumor-infiltrating cytotoxic T lymphocyte (CTL) dysfunction and rejection by immune checkpoints. RNA-sequencing raw count data and corresponding clinical information from the TCGA database were estimated using the TIDE algorithm to predict the potential immunotherapy response. A low score indicated good efficacy.[47] The Spearman microsatellite instability (MSI) score from the TCGA database was analyzed by Spearman.[48]

Gene set enrichment analysis

The bladder cancer cohort of TCGA was divided into high and low CLDN6 expression groups according to the median expression value of CLDN6. The pathways that were enriched by the top ranked genes in the two groups were detected by gene set enrichment analysis (GSEA). For each analysis, the number of gene set permutations was set to 1000. The nominal (NOM) *P* value, false discovery rate (FDR), and normalized enrichment score (NES) were used to identify the pathways enriched in each phenotype.

Immunohistochemistry (IHC)

Paraffin sections were dehydrated in xylene, anhydrous ethanol, 95% ethanol, and 85% ethanol, and then subjected to antigen repair, followed by treatment with UltraSensitive™ SP (Mouse/Rabbit) IHC Kit (KIT-9710, MXB Biotechnology, Fuzhou, China).

For CLDN6, CD163, and NOS2, each tissue sample was scored according to its staining intensity (0, none; 1, weak; 2, moderate; 3, strong) multiplied by the point of the percentage of stained cells (positive cells ≤25% of the cells: 1; 26-50% of the cells: 2; 51-75% of the cells: 3; ≥75% of the cells: 4). The range of this calculation was 0-12. The median value of scores was employed to determine the cut-off. Cancers with scores above the cut-off value were considered to have high expression of the indicated molecule and vice versa.

Western blot (WB)

When cells reach 80% confluence, cells were harvested and washed with PBS. Total protein was extracted with 200 μL RIPA Lysis Buffer (Beyotime, Shanghai, China) with 1 mM phenylmethylsulfonyl fluoride (PMSF) (Sigma, MO, USA) and 1 mM Phosphatase inhibitor (Solarbio, Beijing, China), followed with centrifugation 12,000 g for 20 min. The protein concentration was determined using a BCA Protein Assay Kit (Beyotime, Shanghai, China). 50 μg of denatured protein was applied to 12% SDS-PAGE gels. After electrophoresis the proteins on the gel were then transferred onto a nitrocellulose membrane (Millipore, California, USA). The membrane was blocked with 5% defatted milk at 37°C for 1 h and incubated overnight at 4°C with the primary antibodies. The membrane was incubated with horseradish peroxidase-conjugated secondary antibodies at room temperature for 1 h. Finally, the immunoreactive bands were visualized using an ECL western blotting system (Beyotime, Shanghai, China).

Immunofluorescence (IF)

Cells were fixed with 4% paraformaldehyde and then incubated with 5% BSA. After being incubated with the first antibody at 4°C overnight and following the secondary antibody, the cells were stained with DAPI and visualized with a fluorescence microscope (Olympus, Japan).

Cell counting kit-8 (CCK-8)

Cell viability was measured using CCK-8 reagents (Meilune, China). The cells were seeded in 96-well plates at the density of 1000 cells/well and incubated for 24 h. In each well, a 1:19 diluted CCK-8 solution in DMEM was added and the plates were incubated at 37°C for 2 h in 5% CO2. The absorbance of the sample was measured at 450 nm on a microplate reader (Thermo, Germany).

Plate clone formation assay

The cells were plated into 6-well plates at 600 cells/well in triplicate. The medium was replaced every 2-3 d with a fresh medium until colonies were visible to the naked eye. The colonies were washed and fixed, stained with 5% crystal violet, and then counted.

Medical illustrations

The Figure was partly generated using Servier Medical Art, provided by Servier, licensed under a Creative Commons Attribution 3.0 unported license.

QUANTIFICATION AND STATISTICAL ANALYSIS

Survival differences between groups were assessed using Kaplan-Meier curves and log-rank tests. Prognostic factors were determined with univariate and multivariate Cox regression analyses. Correlation coefficients were calculated by Spearman correlation analyses. Normal and non-normal variables were compared using the unpaired Student t-test and the Mann-Whitney U test, respectively. One-way analysis of variance and the Kruskal-Wallis test were used as parametric and nonparametric methods, respectively, for comparing > 2 groups. The statistical analysis was performed using R software and values represent the mean ± standard deviation. $P < 0.05$ was considered statistically significant. $^{*}P < 0.05$, $^{**}P < 0.01$, $^{***}P < 0.001$.